Esophageal Cancer-Related Gene-4 Contributes to Lipopolysaccharide-Induced Ion Channel Dysfunction in hiPSC-Derived Cardiomyocytes

Qiang Xu [1,2,*], Xiangjie Zhang [3,*], Maolin Hao [3,*], Xitong Dang[3], QianQian Xu [3], Lukas Cyganek[4,5], Ibrahim Akin[2,6], Dan Tang[7], Bin Liao[8], Xiaobo Zhou [2,3,6], Huan Lan [3]

[1]School of Basic Medical Science, Southwest Medical University, Luzhou, People's Republic of China; [2]First Department of Medicine, Faculty of Medicine, University Medical Centre Mannheim (UMM), University of Heidelberg, Mannheim, Germany; [3]Key Laboratory of Medical Electrophysiology, Ministry of Education & Medical Electrophysiological Key Laboratory of Sichuan Province, Institute of Cardiovascular Research, Department of Cardiology, The Affiliated Hospital, Southwest Medical University, Luzhou, People's Republic of China; [4]Stem Cell Unit, Clinic for Cardiology and Pneumology, University Medical Center Göttingen, Göttingen, Germany; [5]DZHK (German Center for Cardiovascular Research), Partner Site, Göttingen, Germany; [6]DZHK (German Center for Cardiovascular Research), Partner Site, Heidelberg, Mannheim, Germany; [7]The First People's Hospital of Longquanyi District, Chengdu/West China Longquan Hospital, Sichuan University, Chengdu, People's Republic of China; [8]Department of Cardiac Macrovascular Surgery, Affiliated Hospital of Southwest Medical University, Luzhou, Sichuan, People's Republic of China

*These authors contributed equally to this work

Correspondence: Huan Lan, Key Laboratory of Medical Electrophysiology, Ministry of Education & Medical Electrophysiological Key Laboratory of Sichuan Province, Institute of Cardiovascular Research, No. 1 section 1 of Xiang Lin Road, Longmatan District, Luzhou City, Sichuan, People's Republic of China, Tel +0086-0830-3160619, Email lanhuan@swmu.edu.cn; Xiaobo Zhou, First Department of Medicine, Faculty of Medicine, University Medical Centre Mannheim (UMM), University of Heidelberg, Theodor-Kutzer-Ufer 1-3, Mannheim, Baden-Württemberg, Germany, Tel +0049-621-3831448, Email Xiaobo.zhou@medma.uni-heidelberg.de

Background and Purpose: Esophageal cancer-related gene-4 (ECRG4) participate in inflammation process and can interact with the innate immunity complex TLR4-MD2-CD14 on human granulocytes. In addition, ECRG4 participate in modulation of ion channel function and electrical activity of cardiomyocytes. However, the exact mechanism is unknown. This study aimed to test our hypothesis that ECRG4 contributes to inflammation-induced ion channel dysfunctions in cardiomyocytes.

Methods: Human-induced pluripotent stem cell-derived cardiomyocytes (hiPSC-CMs) generated from three donors were treated with lipopolysaccharide (LPS) to establish an endotoxin-induced inflammatory model. Immunostaining, real-time PCR, and patch-clamp techniques were used for the study.

Results: ECRG4 was detected in hiPSC-CMs at different differentiation time. LPS treatment increased ECRG4 expression in hiPSC-CMs. Knockdown of ECRG4 decreased the expression level of Toll-Like-Receptor 4 (TLR4, a LPS receptor) and its associated genes and inflammatory cytokines. Furthermore, ECRG4 knockdown shortened the action potential duration (APD) and intercepted LPS-induced APD prolongation by enhancing I_{SK} (small conductance calcium-activated K channel current) and attenuating I_{NCX} (Na/Ca exchanger current). Overexpression of ECRG4 mimicked LPS effects on I_{SK} and I_{NCX}, which could be prevented by NFκB signaling blockers.

Conclusion: This study demonstrated that LPS effects on cardiac ion channel function were mediated by the upregulation of ECRG4, which affects NFκB signaling. Our findings support the roles of ECRG4 in inflammatory responses and the ion channel dysfunctions induced by LPS challenge.

Keywords: esophageal cancer-related gene-4, arrhythmias, lipopolysaccharide, human-induced pluripotent stem cell-derived cardiomyocytes, inflammation

Introduction

Sepsis, caused by severe infection, may result in multiple organ dysfunction, such as heart failure and arrhythmias.[1,2] Lipopolysaccharide (LPS), a key component of the outer membrane of Gram-negative bacteria, is an important

pathogenic factor in sepsis. Heart dysfunction is commonly documented in patients with sepsis and LPS-treated animals.[3,4] LPS in circulation can stimulate the innate immune system and, in turn, leads to a regional or systemic inflammatory reaction. In addition, LPS may activate non-immune cells and evoke inflammation. The LPS receptor, Toll-like receptor 4 (TLR4), has been detected in cardiomyocytes.[5,6] Hence, the innate inflammatory reaction can be stimulated in cardiomyocytes by LPS, without the participation of immune cells. Despite the advancements in the investigation of infection and sepsis, the exact mechanisms of cardiac dysfunctions, particularly arrhythmias, remain to be clarified.

As hiPSC-CMs can be a good platform for modeling cardiac diseases including myocarditis, in our previous study, we established a model of inflammation using hiPSC-CMs challenged by LPS.[7] In this model, we demonstrated that hiPSC-CMs responded to LPS-challenging. The hiPSC-CMs possess LPS-receptor, TLR4, and its associated signaling proteins, including TIRAP, RelA, MyD88 and NFκB1. LPS-treatment induced an increase in proinflammatory factors and chemotactic cytokines in a dose-dependent manner. These results suggested that hiPSC-CMs can be used as a model of inflammation in cardiomyocytes. We also found that hiPSC-CMs challenged by LPS exhibited a prolonged action potential duration (APD). Decreased I_{SK} and increased I_{NCX} contributed to the ADP prolongation. Enhanced I_{NCX} may cause delayed afterdepolarization (DAD), which may lead to tachyarrhythmias. Nevertheless, it is unknown whether LPS directly induces ion channel dysfunction or whether other factors are involved in this process.

ECRG4 was cloned by mRNA differential display between normal and cancerous epithelium of esophagus. It was originally recognized as a tumor suppressor gene.[8] Studies have shown that ECRG4 is constitutively expressed in normal epithelium of esophagus and downregulated in esophageal cancer, and ECRG4 levels are directly correlated with prognosis.[9] Besides epithelium, ECRG4 has been reported to be widely expressed in many other types of cells, including skeletal muscle, cardiomyocytes, pancreatic exocrine cells and hepatocytes.[10] Similar to mouse and rat, in adult human heart, the ECRG4 expression is higher in atrial myocardium than in left ventricular myocardium.[11,12]

ECRG4 expression was documented to be downregulated after injury and infection, similar to its downregulation in tumors.[13–15] Nonetheless, upregulation of ECRG4 gene was observed in chronic inflammation as well.[16,17] In adult human heart, Huang et al detected that the ECRG4 expression level was largely reduced in atrial appendages of atrial fibrillation (AF) patients compared with the sinus rhythm (SR) group. In rat neonatal cardiomyocytes, the knockdown of ECRG4 significantly shortened the APDs and upregulated genes involved in proinflammatory cascades and heart remodeling. These data indicate that ECRG4 may play an important role in the pathogenesis of AF.[18] In agreement with the possible role of ECRG4 in atrial electric remodeling, a significant decrease in ECRG4 level in HL1 cells was observed after 24 hours of rapid electric stimulation.[19] Taken together, ECRG4 may participate in the modulation of ion channel function and electrical activity of cardiomyocytes, but the electrophysiological mechanism is unclear.

In human granulocytes, ECRG4 was found to exist in the innate immunity complex TLR4-MD2-CD14 and modulated inflammation through non-canonical, NFκB signal transduction.[20] Given that LPS can induce arrhythmia through TLR4 receptor, we hypothesize that ECRG4 may contribute to inflammation-induced ion channel dysfunctions in cardiomyocytes. The objective of this study was to evaluate the effects of ECRG4 on LPS-induced ion channel dysfunctions in hiPSC-CMs.

Methods
Ethics Statement
Written consents for skin biopsies, blood and urine were obtained from three healthy donors, from whom three human-induced pluripotent stem cell (hiPSC) lines were generated, respectively. One hiPS cell line was obtained from the University Medical Center Göttingen, and the study plan was approved by the Ethical Committee of the Medical Faculty Mannheim, University of Heidelberg (approval number: 2018–565N-MA), and by the Ethical Committee of University Medical Center Göttingen (approval number: 10/9/15). The other two hiPS cell lines were obtained from Beijing Cellapy Biotechnology Co., LTD with informed consent for scientific research and commercial provision (Cat. No.: CA4025106; CA4027106). The study was performed in accordance with the approved guidelines and fulfilled following the Helsinki

Declaration of 1975, as revised in 1983. The participants gave their written informed consent prior to the study commencing.

Generation of Human iPS Cells

The first cell line UMGi014-B clone 1 (ipWT1.1) of hiPSCs was generated from primary human fibroblasts derived from a skin biopsy. This hiPSC line was generated under feeder-free culture conditions using the integration-free episomal 4-in-1 CoMiP reprogramming plasmid (Addgene, #63726) with the reprogramming factors OCT4, KLF4, SOX2, c-MYC, and short hairpin RNA against p53, as previously described with modifications.[21] The second (B1) and third (U2) hiPS cell lines were generated from primary human blood cells and epithelial cells in urine, respectively. These two hiPSC lines were generated under feeder-free culture conditions using lentiviral particles carrying the transactivator (TA) and an inducible polycistronic cassette containing the reprogramming factors OCT4, SOX2, KLF4 and c-MYC. Generated hiPSCs were cultured under feeder-free conditions and were validated for pluripotency.

Generation of hiPSC-CMs

Frozen aliquots of hiPSCs were thawed and cultured under feeder cell-free condition and differentiated into cardiomyocytes (hiPSC-CMs). Culture dishes and wells were coated with Matrigel (Corning, USA). Culture medium for hiPSCs was TeSR-E8 (Stemcell Technologies, USA), and the medium for hiPSC-CMs was RPMI 1640 GlutaMax (Thermo Fisher Scientific, USA) containing Penicillin/Streptomycin and B27 with and without insulin (Thermo Fisher Scientific, USA). After the third passaging, hiPSC colonies were passaged by Versene solution (Thermo Fisher Scientific, USA) and transferred to feeder-free 24 well plates. When cells were cultured for expansion to 90% −95% confluence, the cardiomyocyte differentiation was initiated. Application of CHIR99021 (Stemcell Technologies, USA) and IWP-2 (Stemcell Technologies, USA) at different time points induced the cells to differentiate into hiPSC-CMs in the first two weeks after the start of differentiation. Beating cardiac colonies can be observed as early as eight days later. In the third week, a selection medium of lactate (Sigma, USA) containing RPMI 1640 medium without glucose and glutamine (WKS, Germany) was used to select cardiomyocytes. From days 40 to 60, the cells were cultured with basic culture medium and were used for further experiments. For patch-clamp measurements, the cardiomyocytes were dissociated from 24 well plates by Collagenase I and plated on Matrigel-coated 3.5 cm petri dishes as single cells.

Real-Time PCR Assays

To measure the mRNA expression in hiPSC-CMs, total RNA was extracted using GeneJET RNA Purification Kit (Thermo Fisher Scientific, USA) which includes DNAse. The RNA was reversed transcribed to cDNA using a high-capacity cDNA reverse transcription kit (Applied Biosystems, USA). cDNA was amplified by real-time PCR on ABI real-time cycler (Applied Biosystems, USA) using QuantiNova^{TM} SYBR Green PCR Kit (Qiagen, Germany) in the presence of forward and reverse PCR primers. Real-time PCR was performed at 95°C for 2 min, followed by 40 cycles of 95°C for 15 sec and 60°C for 30 sec, then followed by melting-curve analysis to verify the specificity of the PCR product. Relative quantification of mRNA expression was calculated by the $\Delta\Delta Ct$ method. Three replicate wells were used for each sample and at least three biological replicates were used for the calculation.

Immunofluorescence Staining

Cardiomyocytes were dissociated from 24 well plates by Collagenase I and TrypLE reagents and plated on Matrigel-coated 8 chamber glass slides (Ibidi, Germany). After at least 48 h, the cells were washed with PBS. For proteins in the intracellular, the cells were fixed with 4% paraformaldehyde (Thermo Fisher Scientific, USA) for 10 min and washed again by PBS. Then, the cells were permeabilized for 10 minutes with 0.5% Triton X-100 (Sigma, USA) and washed with PBS. For cell surface immunofluorescence, Triton X-100 was not used. PBS containing 1% bovine serum albumin (Sigma, USA) was used to block cells for 30 min. After washing with PBS, cells were incubated with primary antibodies in 4°C overnight kept under wet conditions. The next day, cells were washed twice with PBS, and incubated with fluorescent secondary antibodies (Invitrogen, USA). After incubation for 1 h at room temperature, cells were washed twice with PBS. Nuclear staining was performed with ProLong™ gold antifade mountant with DAPI (Invitrogen, USA).

Wheat Germ Agglutinin (WGA) with Alexa Fluor 488 was used for plasma membrane labeling. The antibodies used in this study were α-actinin antibody (Invitrogen, USA), cTnT antibody (Invitrogen, USA), ECRG4 antibody (Sigma, USA) and TLR4 antibody Proteintech, China). Images were taken with Leica DMRE fluorescence microscope (DFC3000G/ DFC 450c) camera equipped with the Leica Application suite 4.4 software.

Construction of Adenovirus for ECRG4 Knockdown and Overexpression

Small RNAs targeting human ECRG4 were designed and used for the ADV1 plasmid (GenePharma, China). The three oligos containing the core siRNA sequences (designated as 230, 388 and 502), targeting ECRG4 coding sequence, were annealed with their corresponding reverse complementary strands and cloned into ADV1, an adenovirus vector co-transcribing GFP downstream of the siRNA precursor. The identity of each plasmid was confirmed by DNA sequencing. Knockdown efficiency was determined by infection with hiPSC-CMs, and the expression of ECRG4 was evaluated by real-time PCR. The siRNA sequence 502 had a better knockdown efficiency and was used in the future experiments. An ADV1 plasmid carrying the full sequence of ECRG4 was used for ECRG4 overexpression. Virus containing a negative siRNA targeting shame RNA was used as a control.

Western Blot Analysis

Following treatment of ECRG4-siRNA and negative control adenovirus to hiPSC-CMs for 48 hours, the cells were lysed at 4°C using lysis buffer containing 25 mm Tris-HCl, pH 8.0, 137 mm NaCl, 2.7 mm KCl, 1% Triton X-100 and protease inhibitor mixture (Thermo, USA) for 1h followed by brief sonication. After 10 min centrifugation at 14,000 rpm at 4°C for removing insoluble materials, supernatants were collected, and the protein concentrations were measured by Pierce™ BCA Protein Assay Kit (Thermo, USA). Equal amounts of whole cell lysates were boiled for 5 min in an SDS-sample buffer, separated by a 10% SDS-PAGE, and electro-transferred onto Immobilon-P membranes (Millipore, Bedford, MA), which were blocked after saturation by TBS-T containing 5% BSA at room temperature for 1 h, and subsequently incubated with the anti-IKK and anti-Phospho-IKK alpha/beta (Affinity, China), anti-NF-kB p65 and Phospho-NF-kB p65 (Affinity, China), anti-GAPDH (Invitrogen, USA) primary antibody, followed by incubation with a secondary horseradish peroxidase (HRP)-conjugated antibody (Cell Signaling, USA). After being washed by TBS-T, the membranes were developed using an enhanced chemifluorescence detection system (Thermo, USA).

Patch-Clamp

Standard patch-clamp whole-cell recording techniques were employed to measure ion channel currents and action potentials (AP). Patch electrodes from borosilicate glass capillaries (MTW 150F; World Precision Instruments, Inc., USA) were pulled by a DMZ-Universal Puller (Zeitz-Instrumente Vertriebs GmbH, Martinsried, Germany). The resistance of pipette electrodes ranged from 4 to 5 MΩ. After the electrode was moved into bath solution, its offset potential was zero-adjusted. After a giga-seal was formed, the fast capacitance of pipette was first compensated, and then the membrane under the pipette tip was broken by negative pressure to establish the configuration of whole-cell recording. To measure the cell capacitance, a 50 ms-voltage pulse from −80 to −85 mV was applied to record the capacitance transient current. The area under the transient current curve was then integrated and divided by 5 mV to obtain the whole-cell capacitance in pF. Next, the series resistance (Rs) and membrane capacitance (Cm) were compensated. The liquid junction potential was not considered. Recording signals were sampled at 10 kHz and filtered at 2 kHz by the Axon 200B amplifier and Digidata 1440A digitizer hardware plus pClamp10.6 software (Molecular Devices, Canada). Depending on features of recorded currents, different voltage clamp protocols were used. To obtain the current density, measured currents were normalized to the membrane capacitance. Current–voltage (I–V) curves were obtained by plotting the current density against voltages. The TTX (tetrodotoxin) sensitive late I_{Na} was measured as the average current from 250 to 400 ms of the depolarization pulse. To separate one type of ion channel current from others, a specific channel blocker was used, and the blocker-sensitive current was analyzed.

AP and Potassium Channel Current Recording

The extracellular solution for the AP and potassium channel current measurements consisted of (mmol/l): 127 NaCl, 5.9 KCl, 2.4 CaCl$_2$, 1.2 MgCl$_2$, 11 glucose, 10 HEPES, pH 7.4 (NaOH). For measuring I$_{to}$, 10 μM nifedipine, 10 μM TTX and 1 μM E-4031 were given into the solution for blocking I$_{Ca-L}$, I$_{Na}$ and I$_{Kr}$. For measuring I$_{Kr}$ and I$_{Ks}$, 10 μM nifedipine, 10 μM TTX and 5 mm 4-AP were applied. The intracellular pipette solution consisted of 10 mm HEPES, 126 mm NaCl, 6 mm KCl, 1.2 mm MgCl$_2$, 5 mm EGTA, 11 mm glucose and 1 mm MgATP, pH 7.4 (KOH). To measure SK channel currents, appropriate amount of CaCl$_2$ was added to obtain the free-Ca^{2+} concentration of 0.5 μM from the calculation by using the software MAXCHELATOR. An ATP-free intracellular pipette solution was used to measure the ATP-sensitive K$^+$-channel current (I$_{KATP}$). To measure I$_{Ks}$, 1 μM of E-4031 was added to block I$_{Kr}$.

To separate I$_{Kr}$ from other potassium currents, the Cs$^+$ currents conducted by the KCNH2 (HERG) channels were measured as I$_{Kr}$. Both the extracellular and intracellular solutions were composed of (mmol/L): 140 CsCl$_2$, 2 MgCl$_2$, 10 HEPES, 10 Glucose, pH 7.4 (CsOH).

Sodium and Calcium Current Recording

The extracellular solution used for measuring peak sodium current was composed of (mmol/l): 20 NaCl, 130 CsCl$_2$, 1.8 CaCl$_2$, 1 MgCl$_2$, 10HEPES, 10 glucose, 0.001 nifedipine, pH 7.4 (CsOH). The intracellular solution was composed of (mmol/l): 10 NaCl, 135 CsCl$_2$, 2 CaCl$_2$, 3 MgATP, 2 TEA-Cl, 5 EGTA, 10 HEPES, pH 7.2 (CsOH).

The extracellular solution used for measuring late sodium current was composed of (mmol/l): 135 NaCl, 20 CsCl$_2$, 1.8 CaCl$_2$, 1 MgCl$_2$, 10 HEPES, 10 glucose, 0.001 nifedipine, pH 7.4 (CsOH). The intracellular solution was composed of (mmol/l): 10 NaCl, 135 CsCl$_2$, 2 CaCl$_2$, 3 MgATP, 2 TEA-Cl, 5 EGTA, 10 HEPES, pH 7.2 (CsOH).

The extracellular solution used for recording I$_{Ca-L}$ was composed of (mmol/l): 140 TEA-Cl, 5 CaCl$_2$, 1 MgCl$_2$, 10 chromanol 293B, 10 HEPES, 0.01 TTX, 2 4-AP, pH 7.4 (CsOH). The intracellular solution was composed of (mmol/l): 10 NaCl, 135 CsCl$_2$, 2 CaCl$_2$, 3 MgATP, 2 TEA-Cl, 5 EGTA, 10 HEPES, pH 7.2 (CsOH).

Sodium-Calcium Exchange Current Recording

The extracellular solution used for measuring I$_{NCX}$ was composed of (mmol/l): 135 NaCl, 10 CsCl$_2$, 2 CaCl$_2$, 1 MgCl$_2$, 10 HEPES, 10 glucose, 0.01 nifedipine, 0.1 niflumic acid, 0.05 lidocaine, 0.02 dihydroouabain, pH 7.4 (CsOH). The intracellular solution was composed of (mmol/l): 10 NaOH, 150 CsOH, 2 CaCl$_2$, 1 MgCl$_2$, 75 aspartic acid, 5 EGTA, pH7.2 (CsOH).

Drugs

E-4031, chromanol 293B, nifedipine, NiCl$_2$, niflumic acid, apamin, LPS, lidocaine and dihydroouabain were from Sigma Aldrich, 4-AP was from RBI, TTX was from Carl Roth, TPCA-1 and QNZ (EVP4593) were from Selleck. E-4031, NiCl$_2$, TTX, 4-AP, apamin, LPS, niflumic acid and dihydroouabain were dissolved in H$_2$O. Nifedipine, chromanol 293B, TPCA-1 and QNZ (EVP4593) were dissolved in DMSO, and lidocaine was dissolved in ethanol. Stock solutions were stored at −20 °C.

Statistics

All the data were displayed as mean ± SEM and were analyzed by the InStat© software (GraphPad, San Diego, USA). Kolmogorov Smirnov test was analyzed to decide whether parametric or non-parametric tests were used. To compare parametric data from multiple groups, one-way ANOVA with Holm-Sidak post-test for multiple comparisons was performed. For non-parametric data, the Kruskal–Wallis test with Dunn's multiple comparisons post-test was used. Unpaired Student's *t*-test was performed to compare two independent groups with normal distribution. $P < 0.05$ (two-tailed) was considered significant.

Results

ECRG4 Was Detected in hiPSC-CMs

To investigate whether ECRG4 is expressed in hiPSC-CMs, we generated hiPSC-CMs from healthy donors and collected total mRNA at different differentiation time. ECRG4 expression on human cardiac muscle cell line AC16 and mice

cardiomyocytes was detected as positive control. Expression levels of ECRG4 were analyzed by real-time PCR. The results showed that ECRG4 was highly expressed in hiPSCs (d0) and mesoblastemas on day 5 of differentiation, and the expression level was largely decreased from day 10, when hiPSC-CMs were generated (cells started to beat). Then, the expression of ECRG4 in hiPSC-CMs increased slightly and was sustained until the maturation stage (Figure 1A).

For verification of the PCR results, we further performed an immunofluorescence study. hiPSC-CMs were stained with α-actinin, cTnT and ECRG4 antibodies with different fluorescent dyes. Nuclear staining was performed with DAPI. Adult mice cardiomyocytes were stained as positive control. As shown in Figure 1B, ECRG4-positive immunofluorescence signal was detected localized to peri-nucleus and cytoplasm and together with cardiomyocytes marker α-actinin and cTnT in hiPSC-CMs, which is the same as adult mice cardiomyocytes (Figure S1A). These results suggest that hiPSC-CMs express ECRG4.
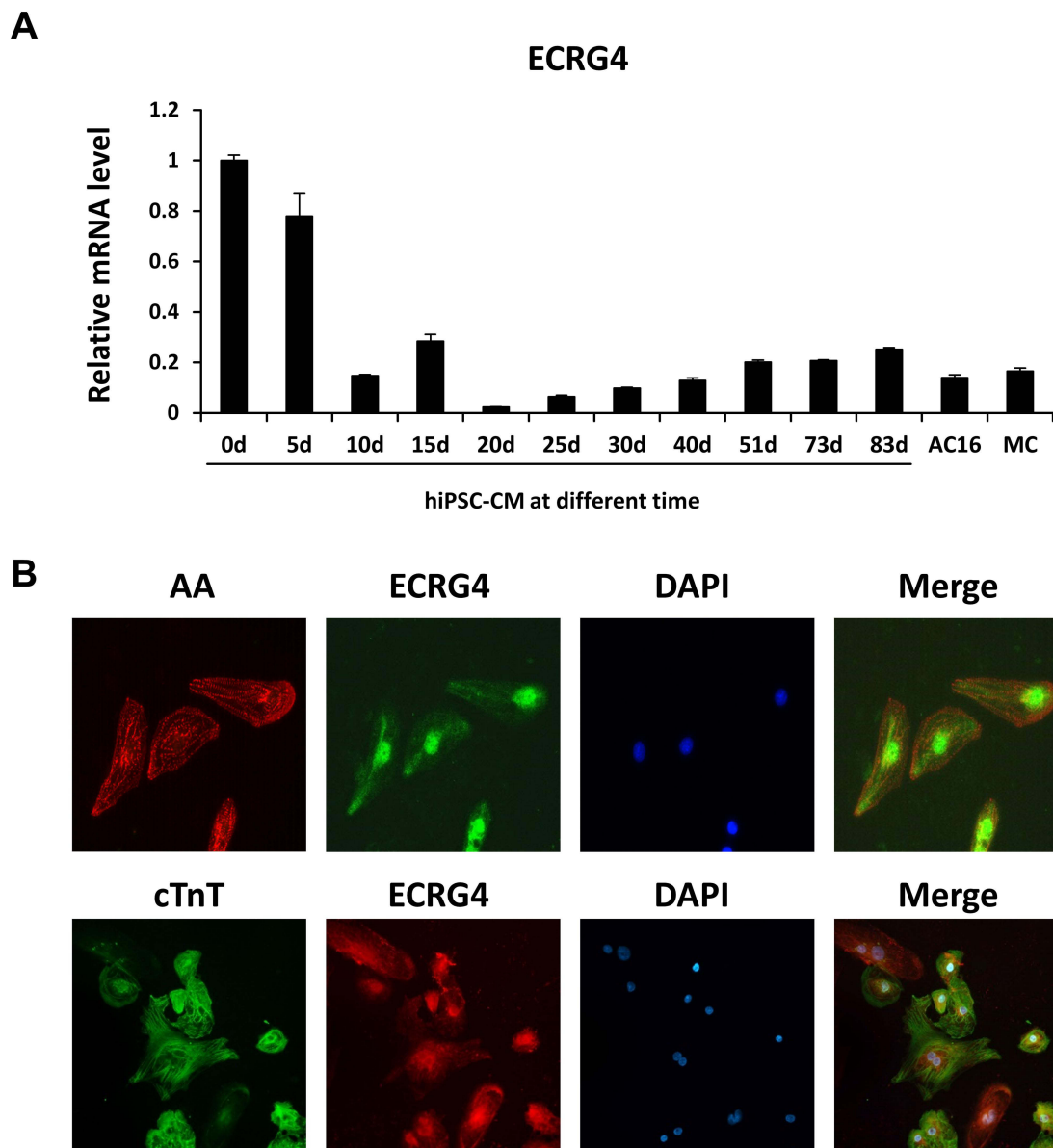
Figure 1 Expression of ECRG4 in hiPSC-CMs (hiPSC-CM-WT1.1) at different differentiation time and immunostaining of hiPSC-CMs for ECRG4. (**A**) Relative mRNA levels (normalized to GAPDH) of ECRG4 were analyzed by real-time PCR in hiPSC-CMs at different differentiation time as well as human cardiac muscle cell line AC16 and mice cardiomyocytes (MC). (**B**) Immunostaining of hiPSC-CMs at day 60 after differentiation with α-actinin, cTnT and ECRG4 antibody, showing the expression of ECRG4 in hiPSC-CMs. Nuclear staining was induced with DAPI (blue).

10188

DovePress

Journal of Inflammation Research 2024:17

LPS Treatment Enhanced ECRG4 Expression Level in hiPSC-CMs

Studies have demonstrated that ECRG4 is present both on the surface and in the cytoplasm of human monocytes and granulocytes, and a physical interaction between ECRG4 and TLR4-MD2-CD14 on human granulocytes has been detected. However, whether ECRG4 had an interaction with TLR4 in hiPSC-CMs was unclear. Therefore, we investigated the localization of ECRG4 and TLR4 by immunocytochemistry and changes in the expression of ECRG4 after LPS treatment at different concentrations and different times in hiPSC-CMs. The results showed that ECRG4 was localized on the surface of non-permeabilized hiPSC-CMs (Figure 2A), and the co-localization of ECRG4 and TLR4 was detected by co-staining of ECRG4 and TLR4 in hiPSC-CMs (Figure 2B). The expression of ECRG4 in hiPSC-CMs was increased by LPS at concentrations from 0.1 µg/mL to 10 µg/mL and at treatment times from 1 h to 24 h in all three cell lines (Figure 2C and D, S1B), suggesting ECRG4 may involve in LPS-induced inflammatory process.
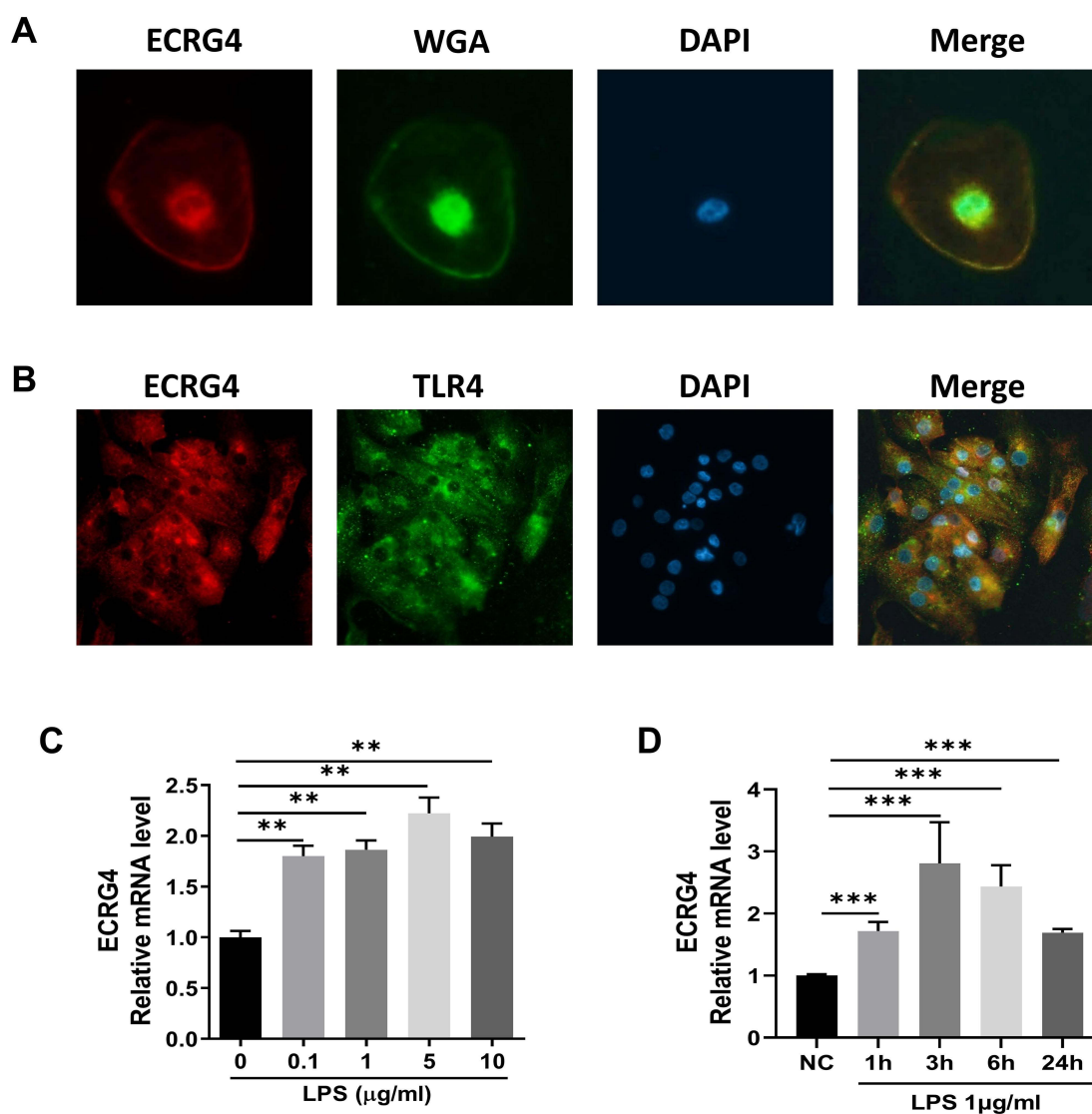

Figure 2 Immunostaining of ECRG4 and TLR4, and expression of ECRG4 in hiPSC-CMs after LPS treatment. (**A**) Immunostaining of non-permeabilized hiPSC-CMs with ECRG4 (red) antibody and WGA (green). Nuclear staining was induced with DAPI (blue). (**B**) Immunostaining for TLR4 (green) and ECRG4 (red) suggest co-localization of TLR4 and ECRG4, which is supported by merged yellow signaling (red + green). Nuclear staining was induced with DAPI (blue). (**C** and **D**) Relative mRNA levels (normalized to GAPDH) of ECRG4 were assessed by real-time PCR in hiPSC-CMs after challenge by LPS at different concentrations for 24 h and different time. Values given are mean ± SEM. ** $P<0.01$, *** $P<0.001$.

ECRG4 Knockdown Changed Expression Level of Toll-Like Receptor 4 Signaling and Ion Channels

To further explore the effect of ECRG4 on inflammatory responses, we first constructed ECRG4-siRNA adenovirus to knock down the ECRG4 expression in hiPSC-CMs, and the knockdown efficiency was verified by real-time PCR. The mRNA level of Toll-like receptor 4 and its associated signaling genes and inflammatory cytokines were analyzed using real-time PCR after ECRG4 knockdown. The result showed that ECRG4-siRNA adenovirus could inhibit about 90% of the ECRG4 mRNA expression (Figure 3A). After ECRG4 knockdown, the expression level of TLR4 and its associated genes, TIRAP, MyD88, MAPK14, MAPK1, MAPK8, IKK2, IKK$_\gamma$, NFκB1, RelA and inflammatory cytokines IL-1β, IL-6 were decreased (Figure 3B and C, S2). Furthermore, Western blot result showed that ECRG4 knockdown decreased the protein level of IKK and NFκB P65 as well as the level of phosphorylated IKK and NFκB P65 (Figure 3D). To investigate the effect of ECRG4 on the ion channels, the mRNA expression of the main ion channels involved in the action potential was measured by qPCR after ECRG4 knockdown. The results showed that the KCNH2 and NCX levels were decreased, but KCNN2 level was increased after ECRG4 knockdown (Figure 3E). These results suggested that ECRG4 is involved in the Toll-like receptor 4 signaling.
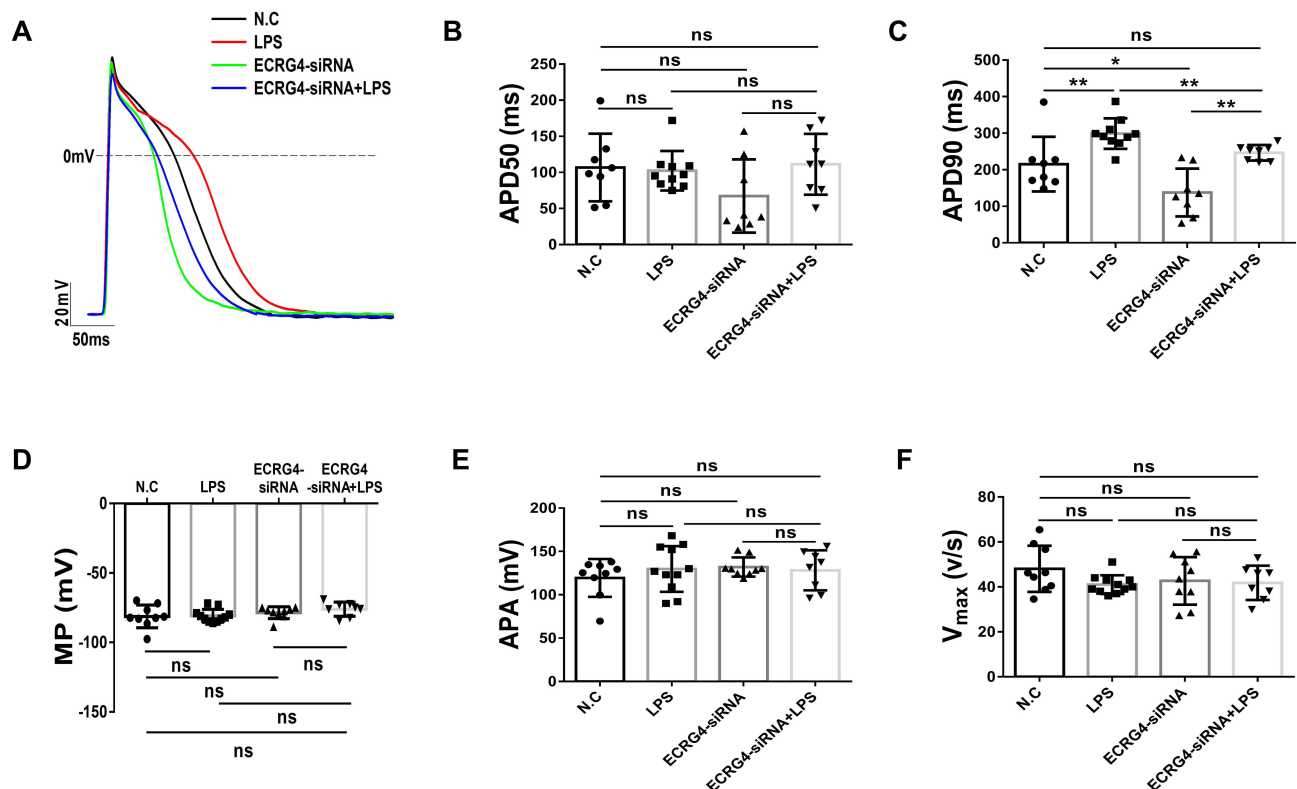
ECRG4 Knockdown Shortened Action Potential Duration (APD) and Intercepted LPS Effect

To further investigate the effects of ECRG4 on the electrophysiological properties of cardiomyocytes and to examine whether ECRG4 is involved in the LPS induced electrophysiological abnormalities, the membrane potentials of hiPSC-CMs with and without ECRG4 knockdown and the negative control were measured in the absence and presence of LPS. In hiPSC-CMs without ECRG4 knockdown, LPS prolonged APD90 (Figure 4C, S3 and S4). ECRG4 knockdown shortened the action potential durations at 90% repolarization (APD90) and prevented the LPS-induced APD-
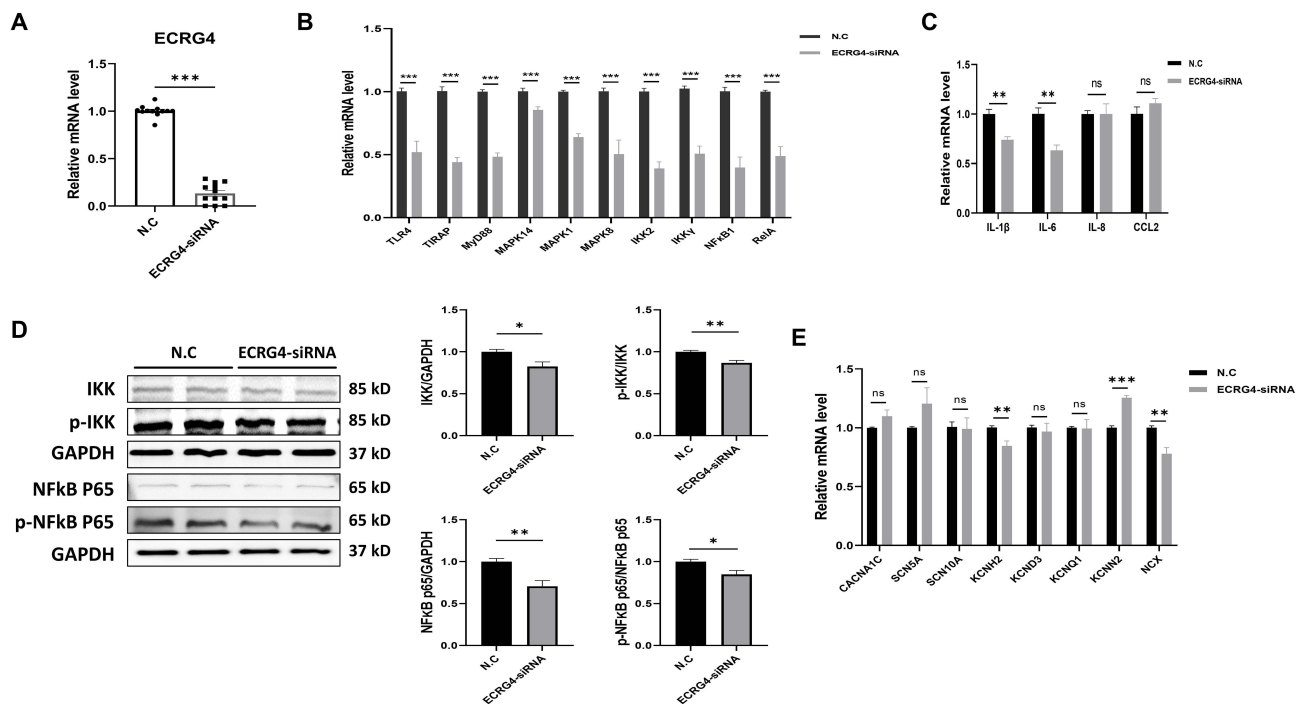
Figure 3 ECRG4 knockdown changes the expression level of TLR4-associated signaling genes, inflammatory cytokines and ion channels in hiPSC-CMs (hiPSC-CM-WT1.1). (**A**) Relative mRNA (normalized to GAPDH) levels of ECRG4 were analyzed by real-time PCR after infection of ECRG4-siRNA adenovirus and negative control (N.C). (**B**) The relative mRNA levels of LPS-signaling associated genes after ECRG4 knockdown. (**C**) The relative mRNA levels of different cytokines after ECRG4 knockdown. (**D**) The Western blot results of total IKK and NFκB P65 (normalized to GAPDH) as well as phosphorylated IKK and NFκB P65 (normalized to total protein) after transfection of ECRG4-siRNA adenovirus and negative control. (**E**) Relative mRNA levels (normalized to GAPDH) of ion channels were analyzed by real-time PCR after transfection of ECRG4-siRNA adenovirus and negative control. Values given are mean ± SEM. *$P<0.05$, **$P<0.01$, *** $P<0.001$ versus control (N.C), ns, not significant.

Figure 4 ECRG4 knockdown shortened potential duration and intercepted LPS effect on APD in hiPSC-CM-WT1.1. (**A**) Representative traces of action potentials (AP) in control, LPS, ECRG4 knockdown and ECRG4 knockdown plus LPS-treated hiPSC-CMs. (**B**) Mean values of APD at 50% repolarization (APD50). (**C**) Mean values of APD at 90% repolarization (APD90). (**D**) Mean values of resting potentials (MP). (**E**) Mean Values of action potential amplitude (APA). (**F**) Mean values of maximal upstroke velocity of AP (Vmax). Values given are mean ± SEM. *$P<0.05$, **$P<0.01$, ns, not significant.

prolongation (Figure 4C, S3 and S4) but did not affect the resting membrane potential (MP), action potential amplitude (APA), the maximal upstroke velocity (V_{max}) and APD50 (Figure 4B–F, S3 and S4). These results indicate that ECRG4 is involved in the LPS induced electrophysiological abnormalities.

ECRG4 knockdown increased small conductance calcium-activated K$^+$ channel currents (I_{SK}) and decreased Na/Ca-exchanger current (I_{NCX})

For analyzing the ion channel currents responsible for the observed changes in APs caused by ECRG4 knockdown, ion channels that may influence APs were assessed. We found that the apamin-sensitive small conductance calcium-activated K+ channel current (I_{SK}) was significantly increased by ECRG4 knockdown (Figure 5 A-C). After ECRG4 knockdown, I_{SK} at 40 mV was increased from 0.4163 ± 0.08 pA/pF to 0.8197 ± 0.14 pA/pF ($P<0.05$). We also observed that the Ni$^+$-sensitive Na/Ca exchanger current (I_{NCX}) was significantly reduced by ECRG4 knockdown (Figure 5 D-F). ECRG4 knockdown reduced I_{NCX} at +60 mV from 1.4363 ± 0.25 to 0.5496 ± 0.06 pA/pF ($P<0.05$) and reduced the current at −100mV, although the change was not statistically significant owing to the large deviation.

Other ion channels that may influence APs, including inward and outward currents, were also assessed. We found that ECRG4 knockdown failed to change the sodium channel currents (peak I_{Na}, Figure S5 A and B), late I_{Na} (Figure S5 C), or L-type calcium channel currents (I_{Ca-L}, Figure S5 D and E). The outward currents of rapidly activating delayed rectifier current (I_{Kr}, Figure S6 A and B), slowly activating delayed rectifier current (I_{Ks}, Figure S6 C and D), transient outward current (I_{to}, Figure S6 E and F), and ATP-sensitive K$^+$ channel current (I_{KATP}, Figure S6 G and H) did not change significantly after ECRG4 knockdown. These results suggested that ECRG4 influence APs through changing I_{SK} and I_{NCX}.
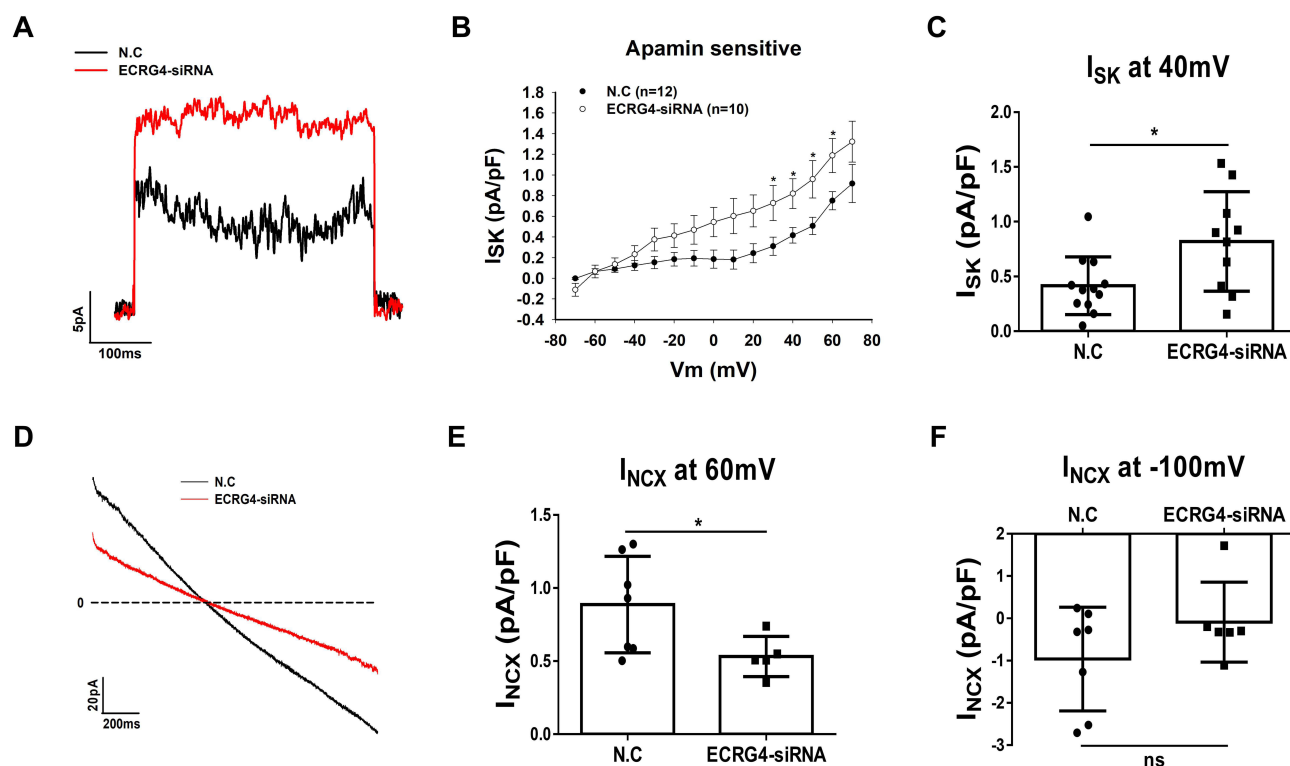
Figure 5 ECRG4 knockdown enhanced small conductance calcium-activated K$^+$ channel currents (I$_{SK}$) and attenuated Na/Ca-exchanger current (I$_{NCX}$) in hiPSC-CM-WT1. 1. Membrane currents were recorded in hiPSC-CMs after transfection of ECRG4-siRNA adenovirus and negative control (N.C). 100 nM apamin, a blocker of SK channels was used to isolate I$_{SK}$ from other currents. The apamin-sensitive currents were analyzed as I$_{SK}$. I$_{NCX}$ was recorded by ramp pulses from −30 to +60 mV, then to −100 mV (100 mV/s) at 0.5 hz with the holding potential of −30 mV. NiCl$_2$ (5 mm) was applied to separate I$_{NCX}$ from other currents. (**A**) Representative traces of apamin sensitive I$_{SK}$ in control and ECRG4 knockdown. (**B**) I–V curves of apamin sensitive I$_{SK}$ from −80 to +80 mV with the holding potential of −50 mV. (**C**) Averaged values of apamin sensitive I$_{SK}$ at +40 mV. (**D**) Representative traces of I$_{NCX}$ in control and ECRG4 knock-down. (**E**) Mean values of peak I$_{NCX}$ at +60 mV. (**F**) Mean values of peak I$_{NCX}$ at −100 mV. Values given are mean ± SEM. *$P < 0.05$, ns, not significant.

ECRG4 Knockdown Could Intercept the LPS Effect on I$_{SK}$ and I$_{NCX}$

To further assess whether inhibition of ECRG4 could reverse the effects of LPS on I$_{SK}$ and I$_{NCX}$, we applied 1 μg/mL LPS for 24 hours to hiPSC-CMs with and without ECRG4 knockdown and then recorded apamin-sensitive I$_{SK}$ and NiCl$_2$-sensitive I$_{NCX}$. We found that LPS increased I$_{NCX}$ and decreased I$_{SK}$, and ECRG4 knockdown could intercept the effects of LPS on I$_{SK}$ and I$_{NCX}$ (Figure 6 A–D, S7 and S8). These results indicated that the effects of LPS on both currents are ECRG4-dependent.

NFκB Signaling Blockers Inhibited the ECRG4 Effect on I$_{SK}$ and I$_{NCX}$

We observed that ECRG4 knockdown decreased the expression level of TLR4 and its associated genes. This suggested that ECRG4 may mediate the effects of LPS through NFκB signaling. To test this hypothesis, a selective blocker, 5-(4-fluorophenyl)-2-ureidothiophene-3-carboxamide (TPCA-1), an inhibitor of the nuclear factor kappa-B kinase sub-unit beta (IKK$_2$) and a NFκB blocker, QNZ (EVP4593) were used together with ECRG4 overexpression adenovirus to detect the effect of ECRG4 on I$_{SK}$ and I$_{NCX}$. As reported before, 0.5 μM TPCA-1 was applied in hiPSC-CMs infected with ECRG4 overexpression adenovirus for 1 hour before current recording,[22] and 100 nM QNZ(EVP4593) was applied in hiPSC-CMs infected with ECRG4 overexpression adenovirus for 24 hours before current recording.[23] The results showed that ECRG4 overexpression significantly increased ECRG4 expression level in hiPSC-CMs (Figure S9). Overexpression of ECRG4 mimicked the effects of LPS on I$_{SK}$ and I$_{NCX}$. TPCA-1 and QNZ(EVP4593) could reverse the ECRG4 overexpression-induced changes in I$_{SK}$ and I$_{NCX}$ at 60 mV in hiPSC-CMs derived from all three donors (Figure 7 A–D, S9 and S10), which indicated that the effect of ECRG4 on I$_{SK}$ and I$_{NCX}$ were through IKK2 and NFκB signaling.
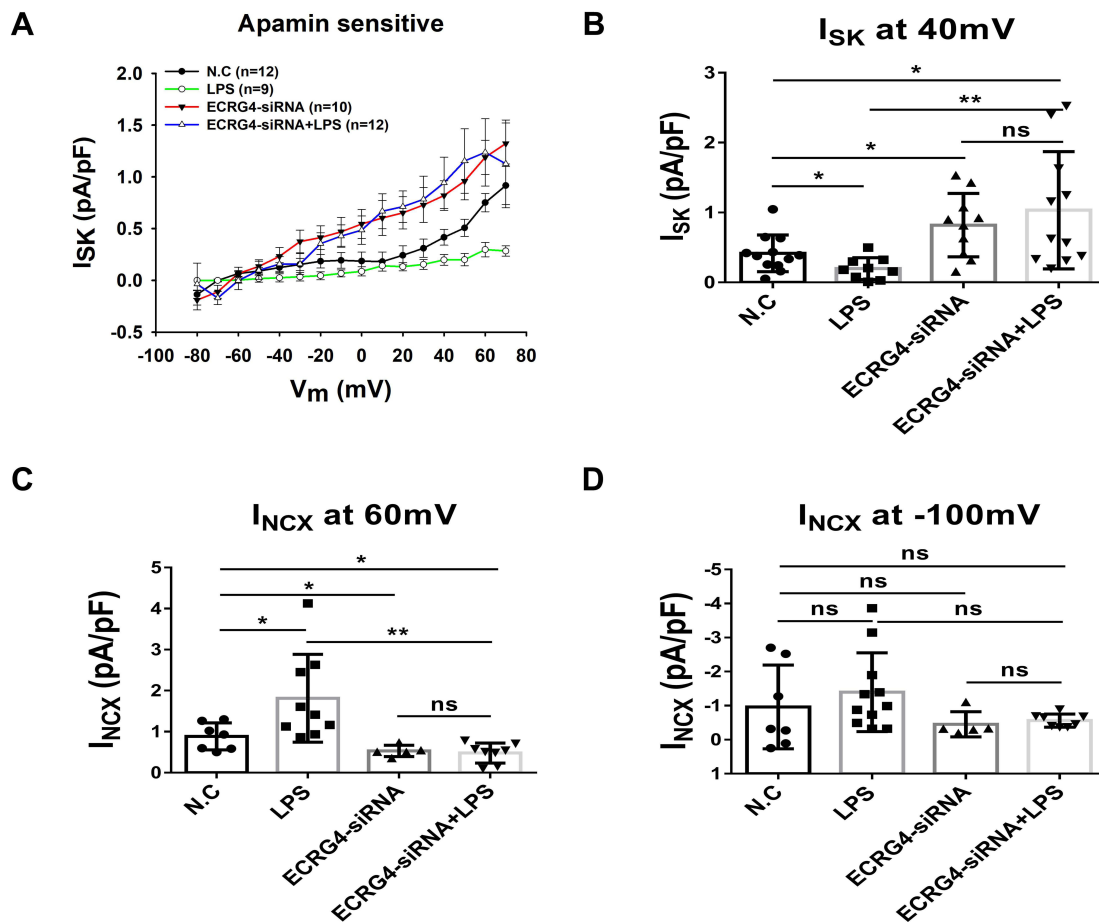
Figure 6 ECRG4 knockdown intercepted the LPS effect on I_{SK} and I_{NCX} in hiPSC-CM-WT1.1. (**A**) Current-voltage (I–V) relationship curves of I_{SK}. (**B**) Mean values of apamin sensitive I_{SK} at +40 mV. (**C**) Mean values of peak I_{NCX} at +60 mV. (**D**) Mean values of peak I_{NCX} at −100 mV. Values given are mean ± SEM. *$P<0.05$, **$P<0.01$, ns, not significant.

Discussion

The connection between inflammation and arrhythmias has been detected for a long time.[24] Severe infections, such as sepsis, may lead to heart dysfunctions, including arrhythmias. Aoki et al reported the role of ion channels in sepsis-induced atrial tachyarrhythmias in guinea pigs.[25] Another study observed that LPS prolonged the action potential duration with enhanced I_{NCX} in isolated rat cardiomyocytes.[26] In HL-1 cells, inflammatory cytokines like TNF can reduce I_{Ca-L} and increase I_{to} and I_{Kur}.[27] In our previous study, we demonstrated that LPS prolonged APD in hiPSC-CMs and the APD prolongation was induced by decreased I_{SK} and increased I_{NCX}, but the mechanism underlying the effects of LPS on both currents was not clarified.

ECRG4 was identified as a tumor suppressor gene. During tumorigenesis, ECRG4 expression is reduced due to hypermethylation of the CpG island in its promoter.[28,29] In addition to traditional epithelial cells, many other cell types, such as chondrocytes, hematopoietic cells, working cardiomyocytes, and atrial-ventricular node also express ECRG4,[30,31] suggesting that ECRG4 has other important functions besides its tumor suppressing role. In fact, it is well-known that an increase in ECRG4 expression has a wide range of effects beyond its antitumor effect, like influencing apoptosis, cell migration, inflammation, injury, and infection responsiveness.

Functions of ECRG4 are also dependent on its cellular localization, secretion, and post-translational processing. Human ECRG4 protein possesses a hormone-precursor-like structure that is sensitive to proteolytic processing. The process can produce different ECRG4-derived peptides, and as many other neuropeptide precursors, each peptide may possess individual, shared, and biologically distinct features depending on proteolytic processing. Previous studies have demonstrated that ECRG4-derived peptides were detectable in lysates of normal tissues, in serum and cerebrospinal fluid,
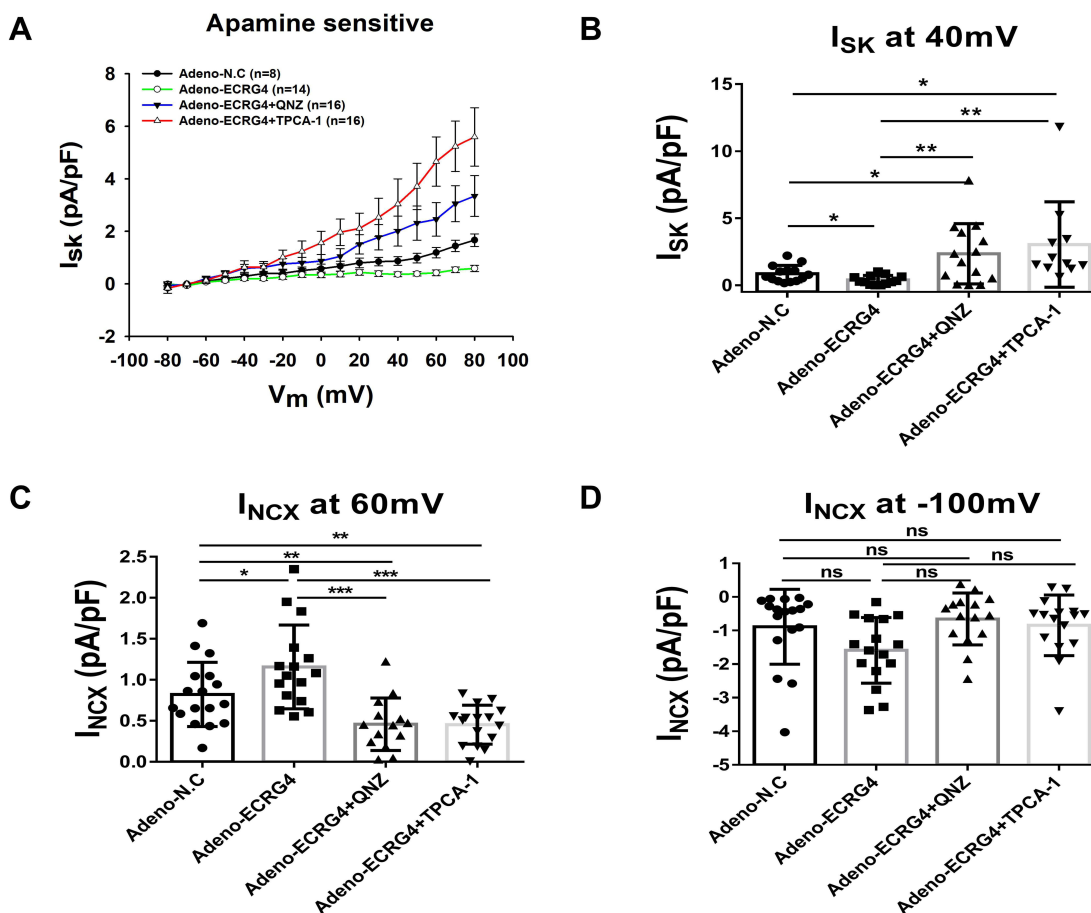
Figure 7 NFκB signaling blockers inhibited the ECRG4 effect on I_{SK} and I_{NCX}. ECRG4 was overexpressed in hiPSC-CMs (hiPSC-CM-WT1.1). TPCA-1 (0.5 μM) was applied 1 hour and QNZ (EVP4593) of 100 nM was applied 24 hours before current recordings in hiPSC-CMs infected with ECRG4 overexpression adenovirus or control virus (N.C). (**A**) Current-voltage (**I–V**) relationship curves of I_{SK}. (**B**) Mean values of I_{SK} at +40mV. (**C**) Mean values of peak I_{NCX} at +60 mV. (**D**) Mean values of peak I_{NCX} at −100 mV. Values given are mean ± SEM. *$P<0.05$, **$P<0.01$, ***$P<0.001$, ns, not significant.

and in the culture media of cells overexpressing ECRG4.[17,32,33] Although ECRG4 is secreted outside the cell, in some cells it is tethered to the cell surface. Upon cell stimulation, peptides produced by ECRG4 processing perform various functions in different types of cells. For example, ECRG4 can participate in both pro- and anti-inflammatory activities, as well as pro- and anti-apoptotic responses.[29,33,34]

Open reading frame mining has identified the interaction of the C-terminal 16 amino acid domain of ECRG4 with the TLR4 immune complex in human granulocytes and may contribute to its effects on inflammation.[20] In hiPSC-CMs, we also identified that ECRG4 was present on the cell surface and the co-localization of ECRG4 and TLR4, suggesting that the ECRG4 may contribute to the inflammation process. Although several reports have shown that ECRG4 is down-regulated in some models of acute injury, we found that ECRG4 was enhanced after LPS treatment at different concentrations in hiPSC-CMs, and the increase occurred shortly after LPS treatment. Tadross et al found proinflammatory functions of ECRG4 peptides, showing that the injection of amino acids 71–148 of ECRG4 into cerebral ventricle elevated the plasma level of adrenocorticotropic hormone and corticosterone in rats.[35] It was also demonstrated that the C-terminal of ECRG4 peptide activated the NFκB signaling in macrophages and interacted with the innate immunity receptor complex (TLR4/CD14/MD2 complex).[14,31] These findings, together with our data showing the upregulation of ECRG4 by LPS stimulation, suggest that ECRG4 can participate in some inflammation relating processes. After knockdown of the ECRG4 in hiPSC-CMs, the expression levels of TLR4 and its associated genes, TIRAP, MyD88, MAPK14, MAPK1, MAPK8, IKK2, IKKγ, NFκB1, RelA and inflammatory cytokines IL-1β and IL-6, were decreased, which indicated that ECRG4 may contribute to gene regulation of LPS/TLR4 signaling.

To explore the role of ECRG4 in ion channel dysfunctions, the expression of ECRG4 was measured at first to prove the existence of ECRG4 in cardiomyocytes. Next, APD and ion channel currents were assessed following ECRG4 knockdown. With ECRG4 knockdown, the expression of KCNH2 and NCX was inhibited, and KCNN2 was enhanced, APD90 was shortened, I_{SK} was increased but I_{NCX} was deceased. These results showed that ECRG4 may participate in the regulation of ion channel functions, and inhibition of ECRG4 may attenuate the LPS effects on ion channel function. In agreement with this hypothesis, the application of LPS in ECRG4-siRNA treated cells failed to prolong the APD and change the I_{SK} and I_{NCX}.

Since LPS treatment increased ECRG4 level, we overexpressed ECRG4 in hiPSC-CMs by transfection with adenovirus carrying ECRG4 gene and measured I_{SK} and I_{NCX} again. Indeed, the overexpression of ECRG4 mimicked the effects of LPS on I_{SK} and I_{NCX}, confirming the contribution of ECRG4 to LPS effect on the channel currents.

Next, we attempted to elucidate the mechanism underlying the effects of ECRG4 on LPS-induced ion channel dysfunctions. IKK2 and NFκB blocker was applied to ECRG4 overexpressing cells. Blockade of NFκB signaling by either an IKK2 blocker or an NFκB blocker could reverse effects of ECRG4 overexpressing adenovirus on I_{SK} and I_{NCX}. These results indicated that ECRG4 effect on ion channels can occur via the NFκB pathway in hiPSC-CMs. IKK2 (IKKβ) is an enzyme that is a component of the cytokine-activated intracellular signaling pathway, the NFκB pathway, which is involved in inflammation and immune responses. It is known that two NFκB pathways exist, depending on the activation of signaling and the cell type, the canonical (IKKβ-dependent) and the noncanonical pathway (IKKα-dependent).[36] Our study shows that the canonical NFκB pathway is involved in ECRG4 affected signaling. Whether the noncanonical pathway is involved needs to be examined in future studies.

In summary, LPS elevated ECRG4 expression level. ECRG4 increased the expression of NCX and decreased the expression of SK channels through TLR4/NFκB/IKKβ signaling. Increased I_{NCX} and decreased I_{SK} contributed to the APD prolongation caused by LPS-ECRG4 signaling.

Conclusion
This study demonstrated that LPS effects on APD, I_{SK} and I_{NCX} were mediated by upregulation of ECRG4, which affects NFκB signaling. Our findings support the roles of ECRG4 in inflammatory responses and the ion channel dysfunctions induced by LPS challenge.

Funding

Disclosure
The authors report no conflicts of interest in this work. Huan Lan and Xiaobo Zhou share the senior authorship. The abstract of this paper was presented at the ESC CONGRESS 2018 name "Esophageal cancer related gene-4 affects multiple ion channel expression in human-induced stem cell-derived cardiomyocytes" as a poster presentation with interim findings. The poster's abstract was published in 'Poster Abstracts' in European Heart Journal, Volume 39, Issue suppl_1, 1 August 2018, ehy563.P3822. The dissertation abstract is also available online at heiDOK – The Heidelberg Document Repository: https://archiv.ub.uni-heidelberg.de/volltextserver/33474/.

References
1. Grune J, Yamazoe M, Nahrendorf M. Electroimmunology and cardiac arrhythmia. *Nat Rev Cardiol*. 2021;18:547–564. doi:10.1038/s41569-021-00520-9
2. Boos CJ. CJ.Infection and atrial fibrillation: inflammation begets AF. *Eur Heart J*. 2020;41:1120–1122. doi:10.1093/eurheartj/ehz953
3. Shahreyar M, Fahhoum R, Akinseye O, Bhandari S, Dang G, Khouzam RN. Severe sepsis and cardiac arrhythmias. *Ann Transl Med*. 2018;6:6. doi:10.21037/atm.2017.12.26

4. Hahmeyer MLDS, da Silva-Santos JE. Hahmeyer MLDS.Rho-Proteins and Downstream Pathways as Potential Targets in Sepsis and Septic Shock: what Have We Learned from Basic Research. *Cells*. 2021;10:1844. doi:10.3390/cells10081844

5. Frantz S, Kobzik L, Kim Y-D. Toll4 (TLR4) expression in cardiac myocytes in normal and failing myocardium. *J Clin Invest*. 1999;104:271–280. doi:10.1172/JCI6709

6. Tavener SA, Long EM, Robbins SM, McRae KM, Van Remmen H, Kubes P. Immune cell Toll-like receptor 4 is required for cardiac myocyte impairment during endotoxemia. *Circ Res*. 2004;95:700–707. doi:10.1161/01.RES.0000144175.70140.8c

7. Yücel G, Zhao Z, El-Battrawy I. Lipopolysaccharides induced inflammatory responses and electrophysiological dysfunctions in human-induced pluripotent stem cell derived cardiomyocytes. *Sci Rep*. 2017;7:2935. doi:10.1038/s41598-017-03147-4

8. Su T, Liu H, Lu S. Cloning and identification of cDNA fragments related to human esophageal cancer. *Zhonghua Zhong Liu Za Zhi*. 1998;20:254–257.

9. Li LW, Yu X-Y, Yang Y, Zhang C-P, Guo L-P, Lu S-H. Expression of esophageal cancer related gene 4 (ECRG4), a novel tumor suppressor gene, in esophageal cancer and its inhibitory effect on the tumor growth in vitro and in vivo. *Int J Cancer*. 2009;125:1505–1513. doi:10.1002/ijc.24513

10. Porzionato A, Rucinski M, Macchi V, Sarasin G, Malendowicz LK, De Caro R. ECRG4 expression in normal rat tissues: expression study and literature review. *Eur J Histochem*. 2015;59:2458. doi:10.4081/ejh.2015.2458

11. Barth AS, Merk S, Arnoldi E. Functional profiling of human atrial and ventricular gene expression. *Pflugers Arch*. 2005;450:201–208. doi:10.1007/s00424-005-1404-8

12. Barth AS, Merk S, Arnoldi E. Reprogramming of the human atrial transcriptome in permanent atrial fibrillation: expression of a ventricular-like genomic signature. *Circ Res*. 2005;96:1022–1029. doi:10.1161/01.RES.0000165480.82737.33

13. Kurabi A. Ecrg4 attenuates the inflammatory proliferative response of mucosal epithelial cells to infection. *PLoS One*. 2013;8:e61394.

14. Podvin S. Esophageal cancer related gene-4 is a choroid plexus-derived injury response gene: evidence for a biphasic response in early and late brain injury. *PLoS One*. 2011;6:e24609.

15. Gonzalez AM, Podvin S, Lin S-Y. Ecrg4 expression and its product augurin in the choroid plexus: impact on fetal brain development, cerebrospinal fluid homeostasis and neuroprogenitor cell response to CNS injury. *Fluids Barriers CNS*. 2011;8:6. doi:10.1186/2045-8118-8-6

16. Steck E, Breit S, Breusch SJ, Axt M, Richter W. Enhanced expression of the human chitinase 3-like 2 gene (YKL-39) but not chitinase 3-like 1 gene (YKL-40) in osteoarthritic cartilage. *Biochem Biophys Res Commun*. 2002;299:109–115. doi:10.1016/S0006-291X(02)02585-8

17. Huh YH, Ryu J-H, Shin S. Huh YH.Esophageal cancer related gene 4 (ECRG4) is a marker of articular chondrocyte differentiation and cartilage destruction. *Gene*. 2009;448:7–15. doi:10.1016/j.gene.2009.08.015

18. Huang LA, Yu H, Fan X. Potential Role of Esophageal Cancer Related Gene-4 for Atrial Fibrillation. *Sci Rep*. 2017;7:2717. doi:10.1038/s41598-017-02902-x

19. Perman JC, Boström P, Lindbom M. The VLDL receptor promotes lipotoxicity and increases mortality in mice following an acute myocardial infarction. *J Clin Invest*. 2011;121:2625–2640. doi:10.1172/JCI43068

20. Dang X, Coimbra R, Mao L. Open reading frame mining identifies a TLR4 binding domain in the primary sequence of ECRG4. *Cell Mol Life Sci*. 2019;76:5027–5039. doi:10.1007/s00018-019-03159-5

21. El-Battrawy I. Modeling Short QT Syndrome Using Human-Induced Pluripotent Stem Cell-Derived Cardiomyocytes. *J Am Heart Assoc*. 2018;7:e007394.

22. Zheng S, Santosh Laxmi YR, David E. Synthesis, chemical reactivity as Michael acceptors, and biological potency of monocyclic cyanoenones, novel and highly potent anti-inflammatory and cytoprotective agents. *J Med Chem*. 2012;55:4837–4846. doi:10.1021/jm3003922

23. Nekrasov ED, Vigont VA, Klyushnikov SA. Manifestation of Huntington's disease pathology in human induced pluripotent stem cell-derived neurons. *Mol Neurodegener*. 2016;11. doi:10.1186/s13024-016-0092-5

24. Vonderlin N, Siebermair J, Kaya E, Köhler M, Rassaf T, Wakili R. Critical inflammatory mechanisms underlying arrhythmias. *Herz*. 2019;44:121–129. doi:10.1007/s00059-019-4788-5

25. Aoki Y, Hatakeyama N, Yamamoto S. Role of ion channels in sepsis-induced atrial tachyarrhythmias in Guinea pigs. *Br J Pharmacol*. 2012;166:390–400. doi:10.1111/j.1476-5381.2011.01769.x

26. Monnerat-Cahli G, Alonso H, Gallego M. Toll-like receptor 4 activation promotes cardiac arrhythmias by decreasing the transient outward potassium current (Ito) through an IRF3-dependent and MyD88-independent pathway. *J Mol Cell Cardiol*. 2014;76:116–125. doi:10.1016/j.yjmcc.2014.08.012

27. Li X, Xue Y-M, Guo H-M. High hydrostatic pressure induces atrial electrical remodeling through upregulation of inflammatory cytokines. *Life Sci*. 2020;242. doi:10.1016/j.lfs.2019.117209

28. Dang X, Zeng X, Coimbra R, Eliceiri BP, Baird A. Counter regulation of ECRG4 gene expression by hypermethylation-dependent inhibition and the Sp1 transcription factor-dependent stimulation of the c2orf40 promoter. *Gene*. 2017;636:103–111. doi:10.1016/j.gene.2017.08.041

29. Baird A, Lee J, Podvin S. Baird A.Esophageal cancer-related gene 4 at the interface of injury, inflammation, infection, and malignancy. *Gastrointest Cancer*. 2014;2014:131–142. doi:10.2147/GICTT.S49085

30. Mirabeau O, Perlas E, Severini C. Identification of novel peptide hormones in the human proteome by hidden Markov model screening. *Genome Res*. 2007;17:320–327. doi:10.1101/gr.5755407

31. Baird A, Coimbra R, Dang X. Cell surface localization and release of the candidate tumor suppressor Ecrg4 from polymorphonuclear cells and monocytes activate macrophages. *J Leukoc Biol*. 2012;91:773–781. doi:10.1189/jlb.1011503

32. Kujuro Y, Suzuki N, Kondo T. Esophageal cancer-related gene 4 is a secreted inducer of cell senescence expressed by aged CNS precursor cells. *Proc Natl Acad Sci USA*. 2010;107:8259–8264. doi:10.1073/pnas.0911446107

33. Dang X, Podvin S, Coimbra R, Eliceiri B, Baird A. Cell-specific processing and release of the hormone-like precursor and candidate tumor suppressor gene product, Ecrg4. *Cell Tissue Res*. 2012;348:505–514. doi:10.1007/s00441-012-1396-6

34. Götze S, Feldhaus V, Traska T. Götze S.ECRG4 is a candidate tumor suppressor gene frequently hypermethylated in colorectal carcinoma and glioma. *BMC Cancer*. 2009;9:447. doi:10.1186/1471-2407-9-447

35. Tadross JA, Patterson M, Suzuki K. Tadross JA.Augurin stimulates the hypothalamo-pituitary-adrenal axis via the release of corticotrophin-releasing factor in rats. *Br J Pharmacol*. 2010;159:1663–1671. doi:10.1111/j.1476-5381.2010.00655.x

36. Israël A. Israël.The IKK complex, a central regulator of NF-kappaB activation. *Cold Spring Harb Perspect Biol*. 2010;2:a000158. doi:10.1101/cshperspect.a000158